

We are IntechOpen, the world's leading publisher of Open Access books Built by scientists, for scientists

5,000

Open access books available

125,000

International authors and editors

140M

Downloads

Our authors are among the

154

Countries delivered to

TOP 1%

most cited scientists

12.2%

Contributors from top 500 universities



WEB OF SCIENCE™

Selection of our books indexed in the Book Citation Index
in Web of Science™ Core Collection (BKCI)

Interested in publishing with us?
Contact book.department@intechopen.com

Numbers displayed above are based on latest data collected.

For more information visit www.intechopen.com



Chapter

Detection of Apoptosis in Cancer Cells Using Heat Shock Protein 70 and p53 Antibody Conjugated Quantum Dot Nanoparticles

Lev B. Matyushkin, Olga A. Aleksandrova, Anna O. Drobintseva, Igor M. Kvetnoy, Yuliya S. Krylova, Yaroslav Y. Marchenko, Dmitriy S. Mazing, Vyacheslav A. Moshnikov, Sergey F. Musikhin, Boris P. Nikolaev, Victoriya O. Polyakova, Maxim A. Shevtsov and Ludmila Y. Yakovleva

Abstract

Clinical experience indicates that enhanced level of heat shock protein 70 (Hsp70) and p53 correlates with poor prognosis due to malignant cell overexpression of these proteins in tumor progression. Cadmium selenide quantum dots (QDs) were synthesized in aqueous solution using mercaptopropionic acid and L-cysteine (L-Cys) as ligands. They were conjugated with a monoclonal antibody (Ab) to p53 and cmHp70.1 to Hsp70 for detection of cancer cell apoptosis that was demonstrated in the experiment by fluorescent confocal microscopy both for breast carcinoma cells and for thyroid tissue. It is shown that in comparison with organic dyes, quantum dots have superior photostability of tracking apoptosis in cancer cells for longer time.

Keywords: quantum dot, p53, heat shock protein, conjugation, cancer imaging

1. Introduction

Imaging is the most powerful diagnostic approach in oncology that provides visualization of early stages of cancer and optimizes its treatment. Fluorescent semiconductor nanoparticles (quantum dots (QDs)) play a great role in cell imaging in oncology [1–3]. QDs have fluorescent characteristics that change conventional approaches in medical diagnostics. The general optical features of QDs compared to organic fluorescent probes are broad excitation band, narrow fluorescence band, high quantum yield (including near-infrared region), and stability against photobleaching [4, 5]. Organic fluorescent dyes are usually used to label cells and tissues for both in vitro and in vivo imaging. QDs are more convenient probes for imaging of tumor cell surface receptors by the receptor-mediated recognition.

Originally proposed back in the early 1990s, synthesis method for colloidal cadmium chalcogenide nanocrystals (CdS, CdSe, CdTe) in high-boiling solvents (the so-called hot injection method) made it possible to carry out controlled synthesis of semiconductor quantum dots with a narrow nanoparticle size distribution and promising optical characteristics [6]. Additional control and modification of optical properties can be achieved using alloying (e.g., Zn_{1-x}Cd_xS QDs) or doping and creation of core-shell heterostructures of type-I (e.g., CdSe/ZnS) or type-II (e.g., CdTe/CdSe) [7, 8]. The technology of colloidal synthesis was extended to other binary compounds, such as lead and silver chalcogenides (for the near-IR range applications), zinc chalcogenides including doped with transition metal atoms (e.g., ZnS:Mn and ZnSe:Mn QDs), III-V semiconductors (InP QDs are actively considered as a less toxic competitor to CdSe-based nanocrystals for the visible range), and group IV semiconductors (e.g., Si, C) [7, 9–12]. Doping of QDs with transition metal ions is a prospective approach for development of bimodal labels for combined magnetic resonance and fluorescence imaging [13]. Another developing system is nanocrystals of ternary I-III-VI compounds (CuInS₂, CuInSe₂, AgInS₂, AgInSe₂), as well as quaternary QDs based on them (e.g., Zn-Ag-In-S QDs) [14, 15]. Being another alternative to cadmium-based nanocrystals in bioimaging applications, they tend to have a common drawback of an inherently broad photoluminescence (PL) band. Some nanocrystalline systems, such as I-III-VI QDs and type-II nano-heterostructures (CdTe/CdSe QDs), with long photoluminescence lifetimes can be used to create fluorescent probes suitable for time-gated imaging with improved signal-to-noise ratio [16]. Despite the fact that the methods of synthesis of colloidal nanocrystals in nonpolar solvents are well studied and allow synthesis of highly fluorescent QDs, methods in aqueous medium attract the attention of researchers due to better cost-effectiveness, relative environmental friendliness, the absence of the need to perform additional operations to hydrophilize the surface of the nanoparticles, and the ability to readily tailor biofunctionality according to specific application. The general restriction to this approach is often higher defect densities and, as a consequence, lower fluorescence quantum yields of nanoparticles. Moreover aqueous synthetic routes may be more complicated due to involvement of H₂O, H₃O⁺, and OH⁻ species [17].

Some proteins are the markers of malignant process and can be used as targeting ligands in imaging. The heat shock protein 70 (Hsp70) and tumor suppressor gene p53 have distinguished position among protein markers. Clinical experience indicates that enhanced level of Hsp70 and p53 correlates with poor prognosis due to malignant cell overexpression of these proteins in tumor progression [18]. Previous studies have shown that these proteins are expressed at high levels in oncological diseases such as endometrial cancers, osteosarcomas, renal cell tumors, hepatoma, and glioblastoma [19, 20]; elevated serum levels of Hsp70 are associated with breast cancer [21]. Hsp70 has prognostic significance for diagnostics of endometrial carcinoma as its expression appears to correlate with sex steroid receptor status in cancer [22].

The wild-type p53 is known to be tumor suppressor apoptotic protein that transcriptionally regulates DNA damage and cell transformation [23]. Interaction of p53 with heat shock proteins changes the apoptotic activity and causes the growth of cancer cells in organism [24, 25]. The Hsp70 is chaperone molecule that affects the p53 function by binding client protein at certain sites. The p53 has two binding sites, the most important one is the C-terminal domain. Therefore, the chaperone function of stress proteins is essential for a sustained state of p53 for malignant cell apoptosis. Targeting of Hsp70 and p53 is an important task for developing the cancer treatment strategy. It is well known that the most sensitive and specific

moieties for detection of antigen are its antibodies (Ab). The conjugation of QDs with monoclonal antibodies against Hsp70 and p53 opens the way for constructing a suitable platform for assay of malignant organs. Nanoparticles ensure delivery and sufficient accumulation of labels in diseased and apoptotic tissues. Targeted delivery of conjugated antibody to a cell membrane receptor was recently demonstrated in the case of magnetic iron oxide nanoparticles. The magnetic conjugates with Ab against Hsp70 being intravenously injected were uptaken by C6 glioma cells [26]. The targeted delivery of magnetic conjugates against epidermal growth factor was confirmed for mouse melanoma. Although the attachment of monoclonal Ab to p53 at the surface of nanoparticle for molecular imaging is not described, the results of successful targeted detection of p53 gene indicate the possibility of apoptosis imaging in transformed cells [27]. Engineered conjugated QDs have diagnostic potential for molecular imaging of apoptosis usually performed by measurement of annexin V bound to phosphatidylserine on an outer cell membrane of tumor [28]. Phosphatidylserine is expressed on the inner side of normal plasma membrane but transfers onto outer leaflet in apoptosis. Some false-positive results in necrosis are the main obstacle for wide application of this assay. Differentiation of apoptosis from necrosis remains an actual problem for oncological diagnostics today. Radiolabeling, magnetic, and QD conjugation do not solve this problem at full scale [29, 30]. As an alternative approach, p53 and Hsp70 proteins in the complex can serve as pro-apoptotic targets for registration with the help of QDs. The QD associated with antibody to pro-apoptotic p53 protein may be used for diagnostic purposes, in particular for the assessment of tumor progression. The apoptotic response after chemotherapy is the special subject for this approach.

In the present study, CdSe QDs were conjugated with monoclonal antibodies to p53 (p53Ab) and cmHp70.1 to Hsp70. The cmHp70.1-QD and p53Ab-QD conjugates were synthesized using covalent bonding. The biocompatibility and cytotoxicity of the obtained conjugates were evaluated by *in vitro* studies in various cancer cell lines C6 glioma, U87 human glioma, K562 human leukemia, and B16 melanoma cells using MTT assay. The imaging potential was evaluated on the breast carcinoma cells by fluorescent confocal microscopy. The use of QD conjugates for expression of cancer marker proteins was also investigated in endometrial and thyroid tissue. The unique photophysical properties of CdSe nanoparticles facilitate the observation of cancer cells by laser confocal microscopy method.

2. Methods

2.1 Reagents

Cadmium chloride ($\text{CdCl}_2 \cdot 2.5\text{H}_2\text{O}$), selenium powder (Se, 99.5%), sodium borohydride (NaBH_4), mercaptopropionic acid (MPA, 99%), and L-cysteine (L-Cys) were used as purchased without further purification.

2.2 Synthesis of CdSe QDs

Typical synthesis procedure included the following steps. Sodium hydroselenide NaHSe solution (Se precursor) was prepared by reacting of NaBH_4 with Se powder in distilled water. It resulted in vigorous reaction accompanied by intensive hydrogen gassing:



To obtain cadmium precursor solution, $\text{CdCl}_2 \cdot 2.5\text{H}_2\text{O}$ was dissolved in distilled water, and the certain amount of MPA was added so that the mixture became turbid. By the dropwise addition of NH_4OH , acidity of the solution was brought up to approximate value $\text{pH} = 11$ and it cleared. It is suggested that moderately alkaline environment facilitates the formation of Cd^{2+} -MPA complexes which act as an immediate reactant. Component molar ratio was adjusted to $[\text{Cd}^{2+}]:[\text{Se}^{2-}]:[\text{MPA}] = 1:0.5:2.4$. Selenium precursor solution was swiftly injected in a solution containing cadmium ions under vigorous stirring at room temperature, followed by rapid heating to 90°C . The QDs were purified by isopropyl alcohol-assisted precipitation and dissolved in phosphate-buffered saline (PBS) buffer. Analogous technique was used to synthesize CdSe QDs capped with L-cysteine.

Luminescence of such particles essentially is associated with radiative recombination via surface states. It is typical for CdSe QDs prepared in an aqueous medium. As compared to QDs, synthesized in an organic medium, such particles have a broader spectrum of luminescence but do not require the additional step of transfer into the aqueous phase. Absorption and photoluminescence spectra are presented in **Figure 1**.

2.3 Characterization of CdSe QDs

The absorption spectra were obtained with ultraviolet-visible-near-infrared spectrophotometer (Ecohim, PE-5400UV) between 190 and 1000 nm, with a spectral resolution of 1 nm. Fluorescence spectra were recorded with a fluorescence spectrophotometer with a solid-state 405 nm laser. Dynamic light scattering (DLS), also known as photon correlation spectroscopy, was used to determine the hydrodynamic diameter of free and conjugated QDs. Diluted samples were used to avoid multiple scattering. The measurements were conducted with Zetasizer (Nano ZS, Malvern Instruments Ltd., UK).

2.4 Evaluation of stability

To assess the stability of the QDs in buffer solutions, CdSe/L-Cys nanoparticles were added in a concentration of $17.5 \mu\text{M}/\text{ml}$ to the following solutions: phosphate-buffered saline, $\text{pH} = 7.5$ (BIOLOT); wash buffer, $\text{pH} = 8.0$ (Dako); and Tris buffer, $\text{pH} = 5.0$ (Sigma). Aliquots of each solution were selected after 60 min, placed on the slides, evaporated, and observed for fluorescent areas using Olympus FV 1000 confocal laser scanning microscope (excitation laser wavelength—405 nm).

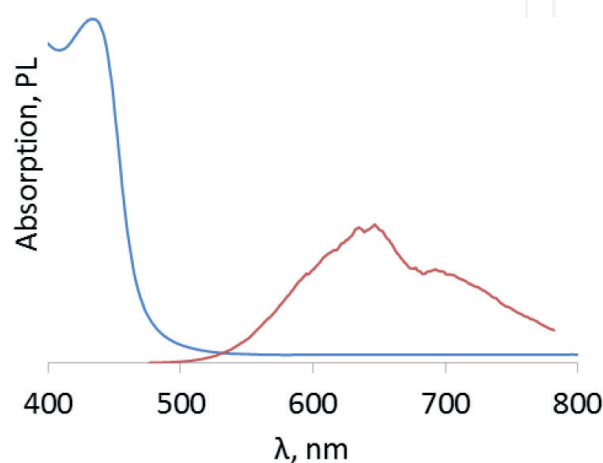


Figure 1. Characterization of the optical absorption and photoluminescence of CdSe nanoparticles.

2.5 Evaluation of fluorescence intensity

The evaluation of the fluorescence intensity of CdSe/L-Cys QDs samples compared to organic fluorophores FITC (rabbit anti-mouse immunoglobulins, conjugated with FITC, Dako) and Alexa Fluor 568 (donkey anti-mouse immunoglobulins, conjugated with Alexa Fluor 568, Abcam) was done in the following way: 15 μl of the fluorophore was added to the slide and mixed with a fluorescence mounting medium (Dako), which prevents the fluorophores from crystallizing and decolorizing, coverslipped, and subjected to ultraviolet radiation (using a Mercury Vapor Short Arc, 120 W) of 25% intensity for 120-min period. A Niba fluorescent filter (for the UV radiation) was used to observe fluorescence. The samples were scanned with the same laser beam intensity every 15 min. The QD sample was irradiated with 405 nm laser, the FITC sample with 488 nm laser, and the Alexa Fluor sample with 559–568 nm laser. The mean fluorescence intensity was measured in relative units using the FluoView 10 software.

2.6 An assessment of the cytotoxic effect of QDs

The cytotoxicity of the CdSe/L-Cys QDs was assessed in two cell cultures. The first cell culture was a cell line ZR-75-1 (breast carcinoma) and the second—normal human mononuclear lymphocytes (MNL).

The apoptosis induction by a fixed staining procedure with propidium iodide (PI) that stains the nuclei of cells with compromised cell membrane structure was determined to assess the cytotoxic effect of QDs in the ZR-75-1 cell line in 1, 3, 18, and 24 h after administration of QD solution.

Phosphate-buffered saline was added as a control in the same quantities to the cell cultures. The QD samples were added to the growth medium at the concentrations of 175 nM/ml, 1.75 $\mu\text{M}/\text{ml}$, and 17.5 $\mu\text{M}/\text{ml}$. The similar method was used to evaluate MNL culture cytotoxic effect, but the concentration of QDs was 1.15 nM/ μl and further evaluated after 48 h of incubation.

2.7 An assessment of the specificity of p53Ab-QD conjugates

The specificity study was conducted with p53Ab-QD conjugate at a 1:50 dilution. The material of the study was normal endometrial cell culture, taken by endometrial pipeline biopsy within the examinations of a patient entering into IVF cycle, as well as fixed and paraffin-embedded thyroid tissue. Endometrial cell culture was grown in Dulbecco's Modified Eagle's Medium (DMEM)/F12 (Gibco) supplemented with 10% fetal bovine serum (Gibco), penicillin, and streptomycin in a humidified atmosphere of 5% CO_2 at 37°C. Apoptosis induction was carried out by adding 200 μM H_2O_2 to the cell culture for 24 h. Normal thyroid tissue possesses a high index of apoptosis. As a control, QD solution of 0.003 M was added in PBS. Immunofluorescence staining was performed using primary antibody (Monoclonal Mouse Anti-Human p53 Protein Clone DO-7, 1:50, Dako) and secondary antibody with Alexa Fluor 647 (Anti-Mouse Alexa Fluor 647, Abcam). The cell nuclei were counterstained with Hoechst stain 33,258 (Sigma); 30 μl volume of each reagent was added per a single slice or well. Fluorescence evaluation was carried out under Olympus FV 1000 confocal laser scanning microscope. The number of stained cells was counted in 10 fields of view at 20 \times magnification.

2.8 Glioma model for Hsp70 assay

Male nu/nu NMRI mice weighing 28–30 g were purchased in animal nursery “Charles River Laboratories” (Germany). All animal experiments have been

approved by the local ethical committee of I.P. Pavlov State Medical University (St. Petersburg, Russia) and were in accordance with institutional guidelines for the welfare of animals.

Animals were anesthetized before mounting in a stereotactic frame (David Kopf Instruments, Tujunga, CA) with 10 mg “Zoletyl-100” (Vibrac sante Animale, France) and 0.2 ml 2% Rometar (Bioveta, Czech Republic) intraperitoneally. U87 cell suspension (1×10^6 cells/ml) in 2 μ l was injected into the nucleus caudatus dexter.

For assessment of the accumulation of the nanoparticles in the tumor, animals were randomly divided into four groups (three animals each) on the 14th day after inoculation: (1) i.v. injection of the PBS (control group); (2) i.v. injection of the QD-Isotype IgG1 for 24 h; (3) i.v. injection of QDs-cmHsp70.1 conjugates for 24 h. Following administration of the QDs, the animals were sacrificed, and extracted brains were fixed in 4% formaldehyde. Brain tumor sections were additionally stained with 4,6-diamidino-2-phenylindole solution (DAPI) (Vector Laboratories, Burlingame, CA, USA). Glasses were mounted in DAKO fluorescent mounting medium (Dako North America Inc., USA) and further analyzed on confocal system. Fluorescence images were captured with a Leica TCS SP5 confocal system (Leica Microsystems, Heidelberg, Germany). For evaluation of co-localization, single z-planes were analyzed with Leica confocal software LCSLite (Leica Microsystems, Heidelberg, Germany) and ImageJ 1.37 (Wright Cell Imaging Facility, Toronto, Canada).

3. Experimental results

3.1 Physical characterization of the CdSe QDs

The optical absorption and fluorescence spectra of the colloidal aqueous solution are shown in **Figure 1**. Absorption band edge around 470 nm is located at energies higher than for the bulk CdSe (bandgap 1.74 eV) proving that grown nanostructures are CdSe QDs. The average diameter of the CdSe QDs can be calculated by inputting the wavelength of the lowest energy absorption peak into the following empirical expression [31]:

$$D = 1.6122 \cdot 10^{-9} \lambda^4 - 2.6575 \cdot 10^{-6} \lambda^3 + 1.6242 \cdot 10^{-3} \lambda^2 - 0.4277 \lambda + 41.57, \quad (2)$$

Here, D (nm) is the mean diameter of the CdSe QDs and λ (nm) is the wavelength of the lowest energy absorption peak, i.e., the first excitonic transition. This expression yielded a diameter of 2 nm, which indicates the formation of ultrasmall QDs. The fluorescence spectrum of the QDs is relatively broad.

3.2 Stability

The carried out observations demonstrated that after the QDs had been incubated in PBS solution and liquid evaporated, the crystalline structure was formed wherein the QDs fluoresce in the orange region of the spectrum. It is found that the QDs remain stable in buffer solutions at room temperature. Herewith the acidity of the solution does not affect the stability of the QDs, since the fluorescence was observed in an hour in all three samples with pH values equal to 8.0, 7.5, and 5.0, respectively. This result is consistent with our previous publication [32].

3.3 Fluorescence intensity of QDs

The comparison analysis of fluorescence intensity of CdSe/L-Cys QDs and organic dyes (**Figure 2**) showed that the maximum brightness of the fluorescence was typical for organic fluorophore FITC in the first 15 min; however, the decrease of brightness (more than threefold) was observed in 15 min. Alexa 568—another organic fluorophore—was more stable than FITC, but its fluorescence intensity also decreased over time. At the same time, the fluorescence intensity of QDs was increasing over time (from 230 to 1000 relative units). Therefore, due to high photostability, QD can be used to monitor fluorescence in objects for long periods of time.

3.4 The assessment of the QD cytotoxicity

The cytotoxicity of the CdSe/L-Cys quantum dots was evaluated using the ZR-75-1 line. The absence of the cytotoxic effect is characteristic for the time intervals of 1, 3, and 18 h. After 24 h, about 4% of cells in the group with injected QDs (concentration of 17.5 mM/ml) accumulated PI, while for the other two groups, these values were 3%. Such a result was not significantly different from the control group, where the number of fluorescent cells scanned was 2 of 100. The number of dead cells in the ZR-75-1 culture did not exceed 3% both in the control and experimental group in all checkpoints. The following results were obtained for a mixed culture of MNL: apoptotic cells were not observed during the first few hours; but long-term (18 h and above) incubation of QDs with MNL proved that the cytotoxic effect increased, and after 48 h, level of apoptosis reached 20%. The increase of cytotoxicity may be associated with the destruction of the organic coating in a cell culture medium. Moreover, MNL were obtained from peripheral blood where lymphocytes do not proliferate without generating special conditions. Therefore, the cytotoxic effect for MNL cell culture may have been more pronounced than for the immortalized ZR-75-1 line. Thus, cytotoxicity was tested both on tumor cells, with greater viability, and on normal human cells, which approximates cytotoxicity assessment for in vivo conditions.

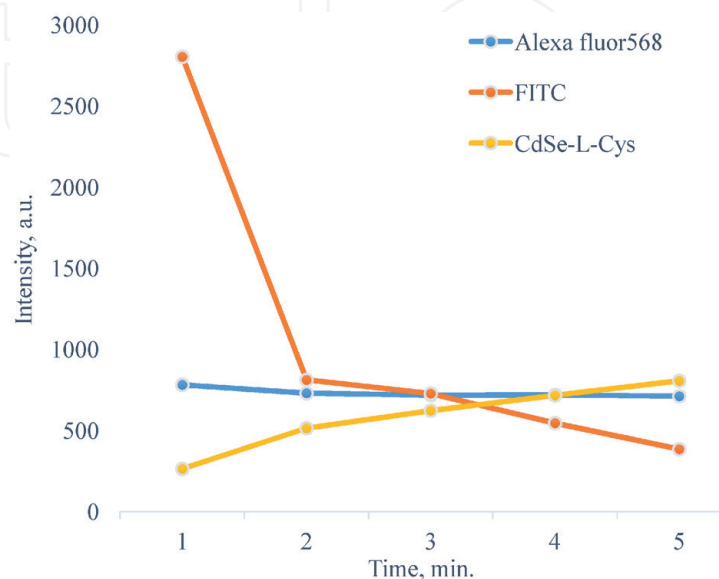


Figure 2.
Dynamic of fluorescence intensity of the CdSe QDs, Alexa Fluor 568, and FITC organic dyes versus time.

3.5 Conjugation of QDs with human antibody against p53 protein (p53Ab)

Conjugation of QDs (CdSe/MPA, 1 mM) and anti-human p53 protein (p53Ab 1:1000 Sigma 0.02 mM) was carried out via water-soluble carbodiimide-mediated linker using CMC (N-Cyclohexyl-N'-(2-morpholinoethyl)-carbodiimide metho-p-toluenesulfonate, Sigma 2 mg/ml (4.7 mM)). 0.2 mM QDs with 0.47 mM CMC was vortexed for 30 min at room temperature. 0.3 μ M or 2.2 μ M p53Ab and 1 \times PBS was added to a final volume 210 μ l. The conjugation of p53Ab with QDs was performed by incubation in the shaker for 3 h after mixing. Nonconjugated QDs without p53Ab were prepared as the control probe. Nonconjugated QDs were removed from the reaction medium by dialysis with size cutoff limit 12–14 kDa. One probe of p53Ab-QD was ultrafiltrated in Vivaspin 100 kDa filter by centrifugation at 10,000 rpm for 3 min. Protein quantity after ultrafiltration and adjustment to a volume of 100 μ l was 0.03 μ M by Bradford assay. The prepared conjugated QDs were stable and had fluorescence as for control solutions. Until use, the conjugates were stored protected from light at 4°C.

Successful conjugation is confirmed by DLS (**Figure 3**). The peak in the size distribution of QD conjugates is shifted toward larger diameters than the case of “free” QDs due to the conjugation with antibodies.

The asymmetry of the distribution in the case of conjugates can be explained by the fact that QDs and antibodies can bind to each other in different proportions. The hydrodynamic diameter of the semiconductor particles is typically larger than the diameter calculated from the absorption spectrum due different physical meaning, but the diameter values are of the same order. The PL spectrum was the same for QDs and their conjugates.

3.6 The specificity of p53Ab-QD conjugates

As a result of specificity assessment experiments for the p53Ab-QD conjugates with apoptosis induced in the cell culture, it was found there were a large number of cell nuclei stained with conjugates (**Figure 4A and C**).

For the evaluation of p53Ab-QD conjugates, we also used a fixed thyroid tissue (**Figure 4B and D**). Such an object of the study was chosen for two reasons: (1) thyroid gland has a high potential of cell renewal (apoptosis index in its parenchyma is about 25%) because of high intensity of synthetic and metabolic processes in normal cells and (2) thyroid pathology often develops during pregnancy and cascade associated with changes in the functioning of the reproductive

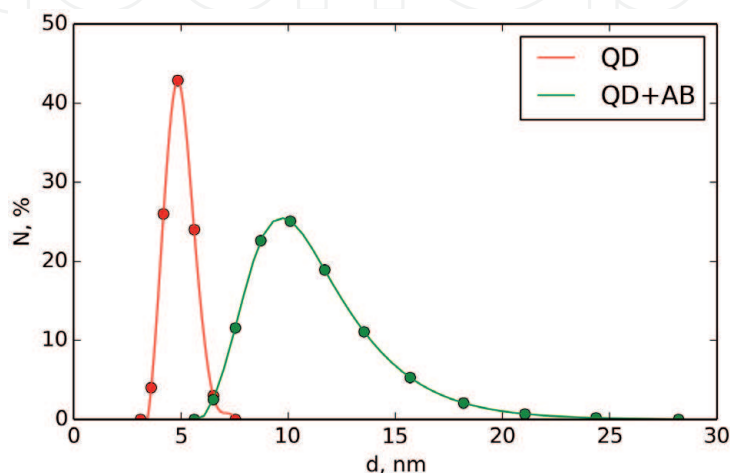


Figure 3.

The size distribution of QDs and QD-p53 antibody in PBS obtained by dynamic light scattering.

system during this period. We observe the expression of the pro-apoptotic protein in the nuclei of thyrocytes.

Thus, the penetration of the p53Ab-QD complexes into the cells was confirmed both in the cell culture and tissue, and specific reaction to the nuclear protein p53 was registered. In comparison with control samples stained with antibodies to p53Ab-Alexa Fluor 647, experimental samples showed a weak fluorescence but sufficient for detection by a confocal microscopy. Stained slides will not discolor over

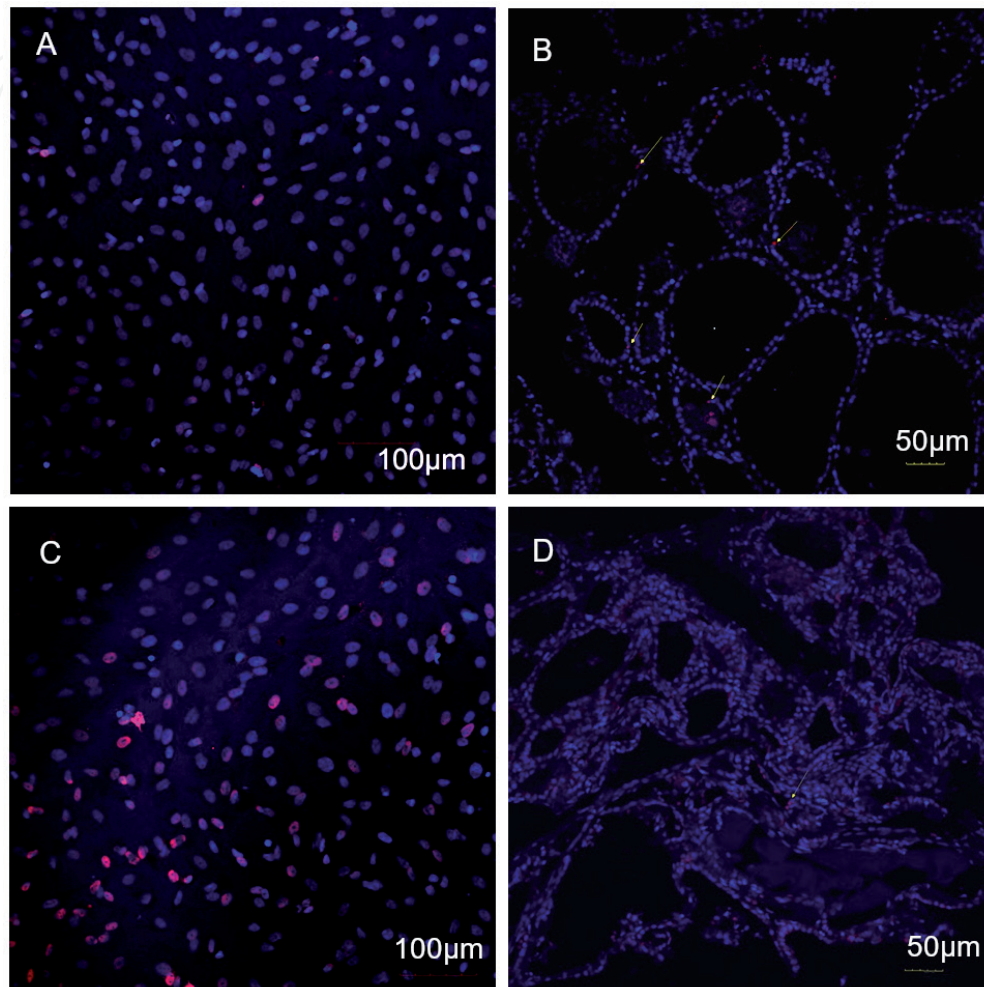


Figure 4. Confocal laser scanning microscopy images. (A) Control, cell culture stained with p53 antibody-Alexa Fluor 647; (B) control, thyroid tissue stained with p53 antibody-Alexa Fluor 647; (C) cell culture with QD-p53 antibody; (D) thyroid tissue with QD-p53 antibody.

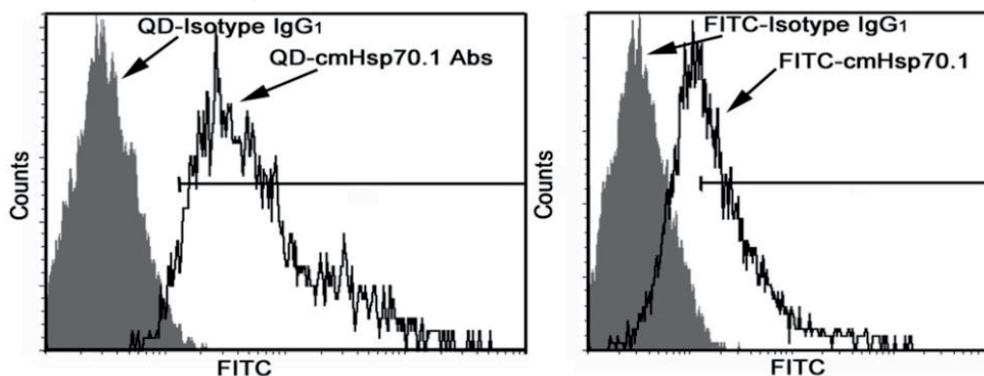


Figure 5. Flow cytometry analysis of Hsp70-positive cells treated by QD-labeled cmHsp70.1 against Hsp70. The results were presented in comparison to fluorescein isothiocyanate-labeled immunoglobulin IgG1.

time, so preservation of the fluorescence intensity was observed at carrying out repeated scans at 1, 3, and 7 days.

3.7 The specificity of cmHsp70.1-QD conjugates

Flow cytometry analysis of Hsp70-positive cells treated by QD-labeled cmHsp70.1 against Hsp70 is shown on **Figure 5**. The results are presented in comparison to fluorescein isothiocyanate-labeled immunoglobulin IgG1.

4. Discussion

The presented above results suggest that CdSe nanoparticles are suitable for constructing the diagnostic platform for attachment of antibodies against proteins actively participating in apoptosis of malignant cells. Heat shock protein 70 in complex with p53 plays important role in apoptotic cell death. Level estimation of these apoptotic proteins can be adapted for monitoring of early stages of cancer. Whether the interaction of Hsp70 and p53 with cancer cells may be registered with high sensitivity by coupling Ab with QD is a subject of the study. For attachment of antibodies against p53 and Hsp70, QDs were synthesized and studied by optical spectroscopy. The core material is semiconductor CdSe nanocrystal coated by short ligands attached to the nanoparticle surface via sulfhydryl groups, while carboxylic groups of the ligands provide sites for conjugation. The study revealed that QDs remain stable for 1 month regardless of the acidity of the buffer solution.

Synthesized QDs have no cytotoxic effect as confirmed by the study of viability not only on tumor cells but also on normal human cells. CdSe/MPA nanoparticles were successfully conjugated with monoclonal antibodies to p53 and cmHp70.1 to Hsp70. The Ab conjugation results in an increase in the hydrodynamic size of nanoparticle from 4.8 nm to 10 nm. The coupling of Ab to CdSe/MPA nanoparticles is carried out without the changes in fluorescence emission spectra of nonconjugated QDs. The strong photoluminescence at $\lambda = 650$ nm allows getting microscopic images unperturbed by background fluorescence of tissues. The amount of Ab per one nanoparticle was similar for Hsp70 and p53 proteins. The covalent coupling of Ab yields random immobilization of Ab at the surface. Some Fab parts of Ab can be in close contact with a surface that restricts immunochemical recognition in ELISA assay. Free access to antigen is determined by chosen synthesis strategy and structure of surface layer. The biological activity depends on the protein density and orientation of Ab on the nanocrystal surface. The large decrease of biological activity follows from a random exposition of epitopes outside of QD [33]. Nonspecific adsorption of conjugated QDs is the additional complication for adequate labeling of apoptotic malignant cells. Experimental data indicate that bioconjugate cmHp70.1-QD shows the specific interaction with cells of C6 glioblastoma line cell. The membrane receptors of C6 cells are appeared to be targeted by QDs coupled with Ab against protein Hsp70. On the basis of experimental data, fluorescent conjugates of Hsp70 are uptaken by surface receptors on abnormal C6 cells. Bioconjugates of QDs for targeted delivery of cancer brain cells were actively studied by numerous researchers. The most known biomolecules for targeted recognition are transferrin, EGFR, some aptamers, RGD peptides, folic acid, etc. Human breast cancer cells and U87MG human glioblastoma cells were robustly labeled by QDs conjugated with RGD peptide [34]. The results of laser scanning confocal microscopy confirm the data earlier obtained for magnetic conjugates SPIONs-Ab-Hsp70 by MRI and NMR methods [26] that QD conjugates are accumulated by C6 glioma cells and brain tumors derived from it. The immunogenic

function of Hsp70 results in an induction of immune response to the association of Hsp70 with cytoplasmic peptides/proteins that translocated out of the cell. It should be noted that the pool of p53 protein is not always recognized by antibody *in vivo* due to its dynamical conformation. p53 protein is an unstable molecule *in vitro*. For prolongation of its lifetime, the presence of heat shock proteins is essential *in vivo*. As regards to the endometrial breast carcinoma cell line ZR-75-1 and p53, the conjugated QDs bound only the surface without internalization in the cell. The bioconjugates retain to some extent the affinity to bind an antigen similar to pure monoclonal antibody. The protein complex from a malignant cell is recognized by the immune system as a foreign antigen. The immunogenic regulation agrees well with anti-apoptotic function Hsp70 as protein affiliated with p53 antitumor activity. The molecular chaperone Hsp70 supports p53 tumor suppressor activity by refolding injured molecules. Overexpression of pair p53-Hsp70 by glioma and breast cancer cells makes possible fluorescent visualization with the help of corresponding Ab-QD conjugates. The obtained results are similar to imaging results of the breast cancer MDA-MB-231 cell line treated by CdSe/CdS core-shell magic-sized QD coupled to a specific breast cancer Fab antibody. But incubation of cancer MDA-MB-231 cells in QD solution was followed by intracellular absorption. Our experiment displays only surface interaction of QDs with cell receptors. The intracellular interaction of the CdSe/p53 conjugates was observed in the fixed tissue thyroid gland. Specific recognition of the nuclear protein p53 was registered as evidence of the expression of the pro-apoptotic protein in the nuclei of thyrocytes.

Engineered conjugated QDs have diagnostic potential for molecular imaging of apoptosis usually performed by measurement of annexin—extracellular phosphatidylserine binding. Proteins p53 and Hsp70 in the complex may serve as pro-apoptotic targets for registration with the help of QDs. The QDs associated with antibody to pro-apoptotic protein p53 may be used for diagnostic purposes, in particular for the assessment of tumor progression. The apoptotic response after chemotherapy is the special subject for this approach.

Acknowledgements

This work was supported by the Russian Science Foundation, project 14-15-00324.

Conflict of interest

The authors declare no conflict of interest.

IntechOpen

Author details

Lev B. Matyushkin¹, Olga A. Aleksandrova¹, Anna O. Drobintseva²,
Igor M. Kvetnoy^{2,3}, Yuliya S. Krylova², Yaroslav Y. Marchenko⁴, Dmitriy S. Mazing^{1*},
Vyacheslav A. Moshnikov¹, Sergey F. Musikhin⁵, Boris P. Nikolaev⁴,
Victoriya O. Polyakova², Maxim A. Shevtsov⁶ and Ludmila Y. Yakovleva⁴

1 Saint-Petersburg Electrotechnical University “LETI”, Saint-Petersburg, Russia

2 Center of Molecular Biomedicine, Saint-Petersburg Research Institute of
Phthisiopulmonology, Saint-Petersburg, Russia

3 Department of Pathology, Saint-Petersburg State University, Saint-Petersburg,
Russia


4 State Research Institute of Highly Pure Biopreparations, Saint-Petersburg, Russia

5 Peter the Great St. Petersburg Polytechnic University, Saint-Petersburg, Russia

6 Institute of Cytology of the Russian Academy of Sciences (RAS),
Saint-Petersburg, Russia

*Address all correspondence to: dmazing@yandex.ru

IntechOpen

© 2020 The Author(s). Licensee IntechOpen. Distributed under the terms of the Creative Commons Attribution - NonCommercial 4.0 License (<https://creativecommons.org/licenses/by-nc/4.0/>), which permits use, distribution and reproduction for non-commercial purposes, provided the original is properly cited. 

References

- [1] Gao X, Cui Y, Levenson RM, Chung LW, Nie S. In vivo cancer targeting and imaging with semiconductor quantum dots. *Nature Biotechnology*. 2004;22:969-976. DOI: 10.1038/nbt994
- [2] Michalet X, Pinaud FF, Bentolila LA, Tsay JM, Doose S, Li JJ, et al. Quantum dots for live cells, in vivo imaging, and diagnostics. *Science*. 2005;307:538-544. DOI: 10.1126/science.1104274
- [3] Radenkovic D, Kobayashi H, Ramsey-Semmelweis E, Seifalian AM. Quantum dot nanoparticle for optimization of breast cancer diagnostics and therapy in a clinical setting. *Nanomedicine: Nanotechnology, Biology and Medicine*. 2016;12:1581-1592. DOI: 10.1016/j.nano.2016.02.014
- [4] Resch-Genger U, Grabolle M, Cavaliere-Jaricot S, Nitschke R, Nann T. Quantum dots versus organic dyes as fluorescent labels. *Nature Methods*. 2008;5:763-775. DOI: 10.1038/nmeth.1248
- [5] Chan WC, Nie S. Quantum dot bioconjugates for ultrasensitive nonisotopic detection. *Science*. 1998;281:2016-2018. DOI: 10.1126/science.281.5385.2016
- [6] Murray C, Norris DJ, Bawendi MG. Synthesis and characterization of nearly monodisperse CdE (E = sulfur, selenium, tellurium) semiconductor nanocrystallites. *Journal of the American Chemical Society*. 1993;115(19):8706-8715. DOI: 10.1021/ja00072a025
- [7] Rogach AL. *Semiconductor Nanocrystal Quantum Dots*. Verlag: Wien; 2008. ISBN: 978-3-211-75235-7
- [8] Zhang Y, Li Y, Yan XP. Aqueous layer-by-layer epitaxy of type-II CdTe/CdSe quantum dots with near-infrared fluorescence for bioimaging applications. *Small*. 2009;5(2):185-189. DOI: 10.1002/smll.200800473
- [9] Yu JS, Kim SH, Man MT, Lee HS. Synthesis and dual-channel optical properties of Mn-doped ZnSe quantum dots. *Materials Letters*. 2019;253:367-371. DOI: 10.1016/j.matlet.2019.07.005
- [10] Silva TG, Moura IM, Filho PEC, Pereira MI, Filho CAA, Pereira G, et al. ZnSe: Mn aqueous colloidal quantum dots for optical and biomedical applications. *Physica Status Solidi (c)*. 2016;13(7-9):530-533. DOI: 10.1002/pssc.201510300
- [11] Hu R, Wang Y, Liu X, Lin G, Tan CH, Law WC, et al. Rational design of multimodal and multifunctional InP quantum dot nanoprobe for cancer: In vitro and in vivo applications. *RSC Advances*. 2013;3(22):8495-8503. DOI: 10.1039/C3RA23169K
- [12] Lee SK, McLaurin EJ. Recent advances in colloidal indium phosphide quantum dot production. *Current Opinion in Green and Sustainable Chemistry*. 2018;12:76-82. DOI: 10.1016/j.cogsc.2018.06.004
- [13] Jing L, Ding K, Kershaw SV, Kempson IM, Rogach AL, Gao M. Magnetically engineered semiconductor quantum dots as multimodal imaging probes. *Advanced Materials*. 2014;26(37):6367-6386. DOI: 10.1002/adma.201402296
- [14] Aldakov D, Lefrançois A, Reiss P. Ternary and quaternary metal chalcogenide nanocrystals: Synthesis, properties and applications. *Journal of Materials Chemistry C*. 2013;1(24):3756-3776. DOI: 10.1039/C3TC30273C
- [15] Xu G, Zeng S, Zhang B, Swihart MT, Yong KT, Prasad PN. New generation

- cadmium-free quantum dots for biophotonics and nanomedicine. *Chemical Reviews*. 2016;**116**(19):12234-12327. DOI: 10.1021/acs.chemrev.6b00290
- [16] Mandal G, Darragh M, Wang YA, Heyes CD. Cadmium-free quantum dots as time-gated bioimaging probes in highly-autofluorescent human breast cancer cells. *Chemical Communications*. 2013;**49**(6):624-626. DOI: 10.1039/c2cc37529j
- [17] Jing L, Kershaw SV, Li Y, Huang X, Li Y, Rogach AL, et al. Aqueous based semiconductor nanocrystals. *Chemical Reviews*. 2016;**116**(18):10623-10730. DOI: 10.1021/acs.chemrev.6b00041
- [18] Luk JM, Lam CT, Siu AF, Lam BY, Ng IO, Hu MY, et al. Proteomic profiling of hepatocellular carcinoma in Chinese cohort reveals heat shock proteins (Hsp27, Hsp70, GRP78) up-regulation and their associated prognostic values. *Proteomics*. 2006;**6**:1049-1057. DOI: 10.1002/pmic.200500306
- [19] Ciocca DR, Calderwood SK. Heat shock proteins in cancer: Diagnostic, prognostic, predictive, and treatment implications. *Cell Stress & Chaperones*. 2005;**10**:86-103. DOI: 10.1379/CSC-99r.1
- [20] Shevtsov MA, Pozdnyakov AV, Mikhrina AL, Yakovleva LY, Nikolaev BP, Dobrodumov AV, et al. Effective immunotherapy of rat glioblastoma with prolonged intratumoral delivery of exogenous heat shock protein Hsp70. *International Journal of Cancer*. 2014;**135**:2118-2128. DOI: 10.1002/ijc.28858
- [21] Kocsis J, Madaras B, Toth EK, Füst G, Prohászka Z. Serum level of soluble 70-kDa heat shock protein is associated with high mortality in patients with colorectal cancer without distant metastasis. *Cell Stress and Chaperones*. 2010;**15**:143-151. DOI: 10.1007/s12192-009-0128-7
- [22] Nanbu K, Konishi I, Mandai M, Kuroda H, Hamid AA, Komatsu T, et al. Prognostic significance of heat shock proteins HSP70 and HSP90 in endometrial carcinomas. *Cancer Detection and Prevention*. 1997;**22**:549-555. DOI: 10.1046/j.1525-1500.1998.00069.x
- [23] Kern SE, Kinzler KW, Bruskin A, Jarosz D, Friedman P, Prives C, et al. Identification of p53 as a sequence-specific DNA-binding protein. *Science*. 1991;**252**:1708-1711. DOI: 10.1126/science.2047879
- [24] Pinhasi-Kimhi O, Michalovitz D, Ben-Zeev A, Oren M. Specific interaction between the p53 cellular tumour antigen and major heat shock proteins. *Nature*. 1986;**320**:182-185. DOI: 10.1038/320182a0
- [25] Hainaut P, Milner J. Interaction of heat-shock protein 70 with p53 translated in vitro: Evidence for interaction with dimeric p53 and for a role in the regulation of p53 conformation. *The EMBO Journal*. 1992;**11**:3513. DOI: 10.1002/j.1460-2075.1992.tb05434.x
- [26] Shevtsov MA, Yakovleva LY, Nikolaev BP, Marchenko YY, Dobrodumov AV, Onokhin KV, et al. Tumor targeting using magnetic nanoparticle Hsp70 conjugate in a model of C6 glioma. *Neuro-Oncology*. 2014;**16**:38-49. DOI: 10.1093/neuonc/not141
- [27] Lim D, Murali R, Murray MP, Veras E, Park KJ, Soslow RA. Morphological and immunohistochemical reevaluation of tumors initially diagnosed as ovarian endometrioid carcinoma with emphasis on high-grade tumors. *The American Journal of Surgical Pathology*. 2016;**40**:302-312. DOI: 10.1097/PAS.0000000000000550
- [28] van Engeland M, Nieland LJ, Ramaekers FC, Shutte B,

Reutelingsperger CP. Annexin V-affinity assay: A review on an apoptosis detection system based on phosphatidylserine exposure. *Cytometry*. 1998;**31**:1-9. DOI: 10.1002/(sici)1097-0320(19980101)31:1<1::aid-cyto1>3.0.co;2-r

[29] Shellenberger EA, Sosnovic D, Weissleder R, Josephson L. Magneto/optical annexin V, a multimodal protein. *Bioconjugate Chemistry*. 2004;**15**:1062-1067. DOI: 10.1021/bc049905i

[30] Lu C, Jiang Q, Hu M, Tan C, Yu H, Hua Z. Preliminary biological evaluation of ¹⁸F-FBEM-Cys-annexin V a novel apoptosis imaging agent. *Molecules*. 2015;**20**:4902-4914. DOI: 10.3390/molecules20034902

[31] Yu WW, Qu L, Guo W, Peng X. Experimental determination of the extinction coefficient of CdTe, CdSe and CdS nanocrystals. *Chemistry of Materials*. 2003;**15**:2854-2860. DOI: 10.1021/cm034081k

[32] Drobintseva AO, Matyushkin LB, Aleksandrova OA, Drobintsev PD, Kvetnoy IM, Mazing DS, et al. Colloidal CdSe and ZnSe/Mn quantum dots: Their cytotoxicity and effects on cell morphology. *St. Petersburg Polytechnical University Journal: Physics and Mathematics*. 2015;**1**:272-277. DOI: 10.1016/j.spjpm.2015.11.003

[33] Mahmoud W, Rousserie G, Reveil B, Tabary T, Millot JM, Artemyev M et al. Advanced procedures for labeling of antibodies with quantum dots. *Analytical Biochemistry* 2011;**416**:180-185. DOI: 10.1016/j.ab.2011.05.018

[34] Cai WB, Shin DW, Chen K, Cheysense O, Cao QZ, Wang SX. Peptide labeled near infrared quantum dots for imaging tumour vasculature in living subjects. *Nano Letters*. 2006;**6**:669-676. DOI: 10.1021/nl052405t